

## INVESTIGATION OF BENDING STRESSES IN ASYMMETRIC INVOLUTE SPUR GEAR BY FEA AND PHOTOELASTICITY

Mr. Dharashivkar N. S. <sup>(1)</sup>

Dr. Vilas.B.Sondur<sup>(2)</sup>

Mr. Krishnakumar D. Joshi<sup>(3)</sup>

<sup>1,2,3</sup>T.K.I.E.T. Warananagar

**Abstract** The work presents a method for investigating the bending stress at the critical section of “Asymmetric Involute spur Gear”. The method ISO/TC- 60 has been used to theoretically calculate the bending stress at the critical section of this Gear. A 3D photoelasticity method has been used to experimentally find out the stress at the critical section of symmetric involute spur gear as well as asymmetric involute spur gear. A comparative analysis between theoretical method, FE method and experimental method to determine bending strength of Asymmetric involute spur gear has been carried out. The percentage increase in bending strength of the Asymmetric gear has been estimated. A substantial weight reduction has been achieved by using asymmetric spur gear instead of symmetric spur gear. Asymmetric gears help to achieve low weight to torque ratio. So, we can build the gearboxes with low weight.

**KeyWords:** Asymmetric gears, Photoelasticity, Bending stress, FEA, ANSYS

### I. Introduction

Gears are the wheels having peripheral teeth around its circumference that engage with another wheel to transmit the motion and hence power. Nowadays, gear design has become a complex and pervasive subject. The process of gear design aims for higher power transmission with a driving system having smaller overall dimensions that can be constructed with optimum cost, low vibration, noise and durability. It is very necessary to revisit the new gear designs in order to enhance the performance requirements like load carrying capacity, endurance strength, speed etc.

The gears are invariably designed to satisfy two main criteria- First is the root bending stress resistance which is analogous to the cantilever effect of tangential load on gear tooth and second one is the flank Hertzian stress resistance which is the resistance of the tooth flanks against the surface rupture when transmitting the tangential load. Fig. 1 shows the failure of gear either by bending stresses or contact stresses.



**Fig. 1 Gear Failure**

The mechanical elements like gears are the well known machine elements that contain sharp or round v-notches. Due to high stress concentration, the notch tip is a likely zone for the initiation of crack and eventually the catastrophic failure of the structures. Thus a good knowledge of the stress distribution around the notch tip is of importance for a reliable evaluation of the load bearing capacity of the notched components. [1, 2, 3]

Adequacy in bending load carrying capacity of a gear unit is a major problem. The critical section of a gear tooth experiences bending stresses that cause most of the failures [4]. The critical section is a section of a gear at which the fillet of a tooth commences. The Critical Section is the shortest distance between starting point of the drive side fillet and that of Coast side fillet. In fig.2 ‘S<sub>f</sub>’ shows the critical section.

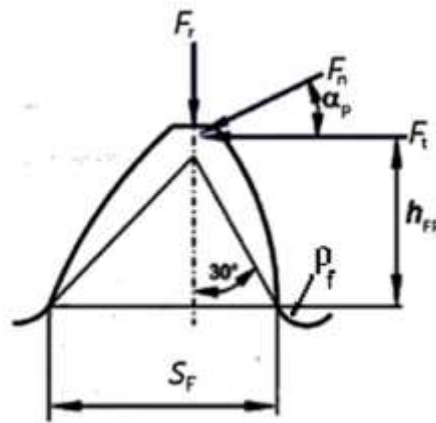


**Fig. 2 Tooth model for Bending stress analysis**

To improve load carrying capacity of a gear tooth, several ways have been suggested such as heat treatment, surface enhancement and modification of tooth geometry.

The work presented in this paper proposes asymmetric profile for spur gears which gives increase in its critical section that results in higher bending strength of gear tooth. This helps to reduce the weight to torque ratio of gearbox.

It is observed that over 90% of all power gear trains have only one main direction for torque transmission [5]. Therefore gear experiences only one directional loading. As the loading is unidirectional, it is not expected for the drive side to be symmetric with coast side which permits the designers to design the gears with asymmetric teeth [6]. These gears provide suppleness to the designers due to non standard geometry of gear tooth. If designed intelligently, these gears can make important contributions to the improvement of designs in aerospace industry, automobile industry, marine drives and wind turbine industry, where weight to torque ratio plays a critical role [7]. Due to their geometry, these gears allow for selection of different pressure angles on drive side and coast side, which is very crucial in obtaining key properties, such as high load carrying capacity and low weight. The high pressure angle on drive side enables to reduce the bending stresses as well as contact stresses where as low pressure angle on drive side helps to reduce the bending stresses and keep the contact stresses on the same level as for symmetric teeth.

### 1.1 Analytical representation of asymmetric involute spur gear

An involute gear is based on an involute curve which is a mathematical shape. There are two key parameters that control the involute curve, the diameter of the cylinder and the angle that the string is unwrapped through, round the cylinder. The string is unwrapped by  $90^\circ$  around the cylinder. The equations for  $90^\circ$  of one full involute have been developed. In other words, the string is unwrapped  $90^\circ$  around the cylinder in a counter clockwise direction [8] [9].

### 1.2 Involute curve for Drive side

The involute curve is defined in Cartesian co-ordinates x-y. In Fig.3, the line S is of the same length as the part of the circumference, the string has been unwrapped by ( $S'$ ) and the instantaneous angle of unwrap is  $\theta_d$  and it changes from  $0^\circ$  to  $90^\circ$ .

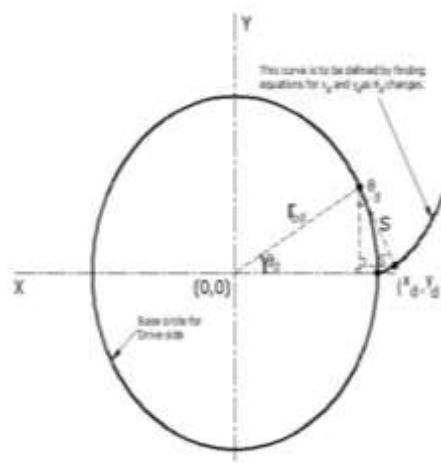


**Fig. 3 Involute curve for Drive side**

We have

$$S' = r_{bd} \times \theta_d \quad (1)$$

But,  $S = S'$ , therefore,

$$S = r_{bd} \times \theta_d \quad (2)$$

The variable  $\theta_d$  determines the current points on the involute curves ( $X_d$ ,  $Y_d$ ). The co-ordinates ( $X_d$ ,  $Y_d$ ) of the considered point on the drive side gear tooth profile are obtained as,

$$X_d = r_{bd} \times (\cos \theta_d + \theta_d \times \sin \theta_d) \quad (3)$$

$$Y_d = r_{bd} \times (\sin \theta_d - \theta_d \times \cos \theta_d) \quad (4)$$

### 1.3 Involute curve for Coast side

The variable  $\theta_c$  determines the current points on the involute curves ( $X_c$ ,  $Y_c$ ). The starting point on the drive and coast side involute curves makes an angle  $\sigma$ , given by

$$\sigma = \text{inv} \alpha_d + \text{inv} \alpha_c + \pi/z \quad [10] \quad (5)$$

In Fig.4, the line  $S$  is the same as the part of the circumference, the string has unwrapped by ( $S'$ ) and the instantaneous angle unwrapped is  $\theta_c$  which increases from  $0^\circ$  to  $90^\circ$ .

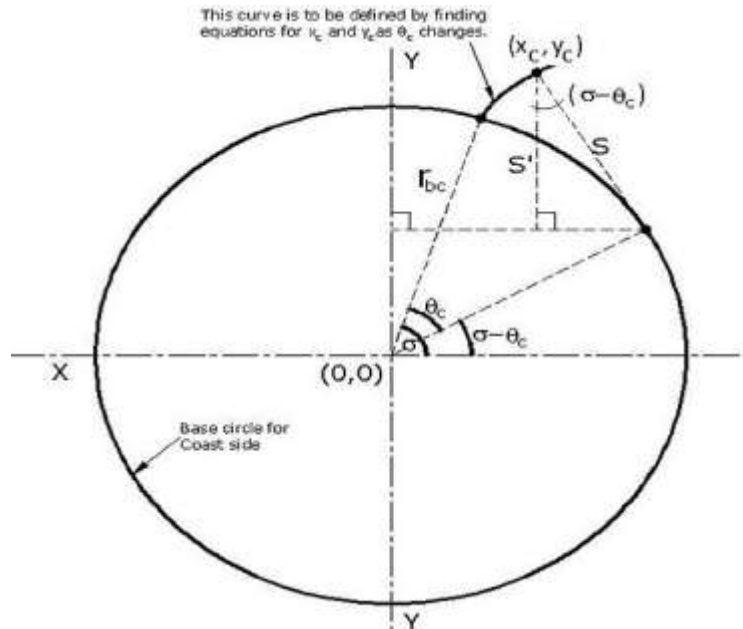


Fig. 4 Involute curve for Coast side

$$S' = r_{bc} \times \theta_c \quad (6)$$

But,  $S = S'$ , therefore,

$$S = r_{bc} \times \theta_c \quad (7)$$

Using trigonometry, co-ordinates  $X_c$  and  $Y_c$  of the considered point on the coast side gear tooth profile are obtained as,

$$X_c = r_{bc} * [\cos(\sigma - \theta_c) - \theta_c * \sin(\sigma - \theta_c)] \quad (8)$$

$$Y_c = r_{bc} * [\sin(\sigma - \theta_c) + \theta_c * \cos(\sigma - \theta_c)] \quad (9)$$

## II. Geometry

Asymmetric gear drives are preferred over symmetric gears as they have more power transmission capacity, lower noise and vibration level. Symmetric gears have same pressure angle for drive side and coast side. There is only one base circle for both the profiles. Since asymmetric gears constitute different pressure angles at drive and coast side, there are separate base circle radii for drive and coast side [11]. Fig.5 shows the geometry of asymmetric gear tooth profile. [10]

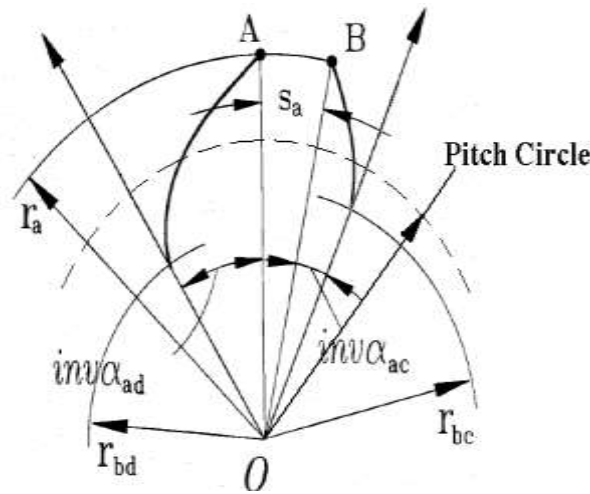


Fig. 5 Drive and Coast side profiles for Asymmetric Spur gear[7]

The pitch circle diameters of pinion and gear,

$$d_1 = m_n \times z_p \quad (10)$$

$$d_2 = m_n \times z_g \quad (11)$$

Centre distance between pinion and gear,

$$CD = \frac{m_n}{2} (z_p + z_g) \quad (12)$$

Radii of base circle on Drive side of Pinion,

$$r_{bd} = \frac{d_1}{2} (\cos \alpha_d) \quad (13)$$

Radii of base circle on Coast side of Pinion,

$$r_{bc} = \frac{d_1}{2} (\cos \alpha_c) \quad (14)$$

Radii of base circle on Drive side of Gear,

$$R_{bd} = \frac{d_2}{2} (\cos \alpha_d) \quad (15)$$

Radii of base circle on Coast side of Gear,

$$R_{bc} = \frac{d_2}{2} (\cos \alpha_c) \quad (16)$$

The tooth thickness at addendum,

$$S_a = r_a \left( \frac{\pi}{z} + (\text{inv} \alpha_c + \text{inv} \alpha_d) - (\text{inv} \alpha_{ac} + \text{inv} \alpha_{ad}) \right) \quad (17)$$

Contact Ratio,

$$CR = (\sqrt{r_a^2 - r_{bd}^2} + \sqrt{R_a^2 - R_{bd}^2} - CD \sin \alpha_d) / (p \times \cos \alpha_d) \quad (18)$$

### III. Bending Stress analysis of Symmetric and Asymmetric involute Spur gear by Theoretical Method

So far, no standard method has been developed to determine the bending stress of asymmetric gear. Pedrero et.al [4] have developed an empirical method for bending stress analysis of asymmetric spur gear based on the recommendations of technical committee ISO/TC- 60. These standards are based on following assumptions:

1. The compressive stress produced by radial component of the load can be neglected.
2. The critical section of the tooth is defined by the point of tangency with a root fillet of a line rotated  $30^\circ$  from the tooth centre line (fig.2).
3. The tooth load acts at the tip of tooth only.

According to DIN-3990, the maximum tooth bending stresses [12] [13]

$$\sigma_{FO} = \frac{F_t}{m_n b} Y_{FP} Y_{SP} \quad (19)$$

Where,

$F_t$	Tangential load acting at the tip of the tooth in N
$b$	Face width of gear in mm
$m_n$	Normal module in mm
$Y_{FP}$	Tooth form factor
$Y_{SP}$	Stress concentration factor

The tooth form factor is defined by,

$$Y_{FP} = \frac{6 \cos \alpha_P \left( \frac{h_{FP}}{m_n} \right)}{\cos \alpha_d \left( \frac{S_F}{m_n} \right)^2} \quad (20)$$

And the stress concentration factor is defined by

$$Y_{SP} = \left( 1.2 + 0.13 \frac{S_F}{h_{FP}} \right) \left( \frac{S_F}{2\rho_F} \right)^{\frac{1}{1.21+2.3 \frac{h_{FP}}{S_F}}} \quad (21)$$

$Y_{SP}$  and  $Y_{FP}$  are the functions of many parameters such as Tool geometry, addendum, tool addendum factor, etc.  $Y_{SP}$  and  $Y_{FP}$  factors greatly depend upon tooth thickness at critical section and distance  $h_{fp}$  from Critical section to the intersection of the tooth centreline and the line of action for load at tip of tooth and the curvature radius  $\rho_f$  at root trochoid as shown in Fig. 2.

The following inputs have been considered for theoretical analysis of Asymmetric Involute Spur Gear and symmetric involute spur gear.

Power transmitted P	10 kW
Pinion rpm $n_p$	1440 rpm
Module $m_n$	3mm
Torque transmitted by pinion	66318 N-mm
Tangential force on gear	1579 N
Number of teeth on pinion $z_p$	28
Number of teeth on pinion $z_g$	42
Tool addendum factor $h_{ao}$	1.25
Material used	Steel-EI-415 [7]
Modulus of elasticity E	$2 \times 10^5 \text{ N/mm}^2$
Poisson's ratio	0.3
DESIGN I: Current Symmetric Gear Set	
Drive side pressure angle $\alpha_d$	$=20^\circ$
Coast side pressure angle $\alpha_c$	$=20^\circ$

DESIGN II: Asymmetric Gear Set

Drive side pressure angle $\alpha_d$	$=25^\circ$
Coast side pressure angle $\alpha_c$	$=20^\circ$

DESIGN III: Asymmetric Gear Set

Drive side pressure angle $\alpha_d$	$=30^\circ$
Coast side pressure angle $\alpha_c$	$=20^\circ$

For all above three designs, face width considered for analysis is 25 mm.

#### IV. A Computer Program

A computer program in C++ has been developed to investigate the variation of bending stress and contact ratio depending upon the pressure angle on the drive side. Regula Falsi method has been adopted to find out thickness at the critical section. Fig. 6 shows a sample output of C++ program. Input parameters mentioned above have been adopted to calculate different parameters required to evaluate the bending stresses. The limiting values here are the tooth thickness at addendum which should be greater than or equal to 0.2 times the normal module and the contact ratio which should be greater than 1.1 for smooth functioning of Gear boxes. These facts have been considered while developing this C++ Program. With reference to Fig. 6, it is seen that bending stresses in asymmetric gear are markedly reduced compared to symmetric gears.

alpha_d	alpha_c	ZP	Y*	HFPD	Sf	Sa	sig_b	Contratio
Drive Side	Coast Side	No. of Teeth	Tooth Factor	mm	Critical Thick.(mm)	Addendum Thick.(mm)	Bend.Stress (N/mm2)	
20	20	28	4.13	5.7	6.15	2.19	87.03	1.68
25	25	28	3.71	5.86	6.72	1.63	78.07	1.49
30	30	28	3.32	6.05	7.38	0.99	69.89	1.36
35	35	28	3.00	6.34	8.13	0.25	63.09	1.29
22	20	28	4.05	5.74	6.26	2.00	85.16	1.60
24	20	28	3.99	5.84	6.37	1.97	84.07	1.52
26	20	28	3.91	5.89	6.5	1.85	82.33	1.46
28	20	28	3.83	5.96	6.63	1.72	80.68	1.41
30	20	28	3.76	6.05	6.76	1.59	79.12	1.36
32	20	28	3.69	6.15	6.91	1.45	77.65	1.33
34	20	28	3.62	6.27	7.06	1.30	76.28	1.3
36	20	28	3.56	6.42	7.22	1.14	75.01	1.28
38	20	28	3.51	6.59	7.39	0.98	73.83	1.26
40	20	28	3.46	6.8	7.57	0.8	72.76	1.25
42	20	28	3.41	7.04	7.76	0.61	71.78	1.24

Fig. 6 Sample output of C++ program

Although, symmetric gear with increased pressure angle gives minimum bending stresses they are not used as they become very rigid and leads to increased vibration level. Besides reducing the pressure angle on coast side makes gear teeth more flexible absorbing the tooth engagement impact and reduction of vibration level.

The various critical parameters like Bending Stresses, Contact Ratio, Critical section thickness and Tooth tip thickness at addendum circle have been plotted against the Pressure angle on Drive side of the tooth profile for asymmetric gear. Figures 7, 8, 9 and 10 show the variation of these critical parameters against the drive side pressure angle.

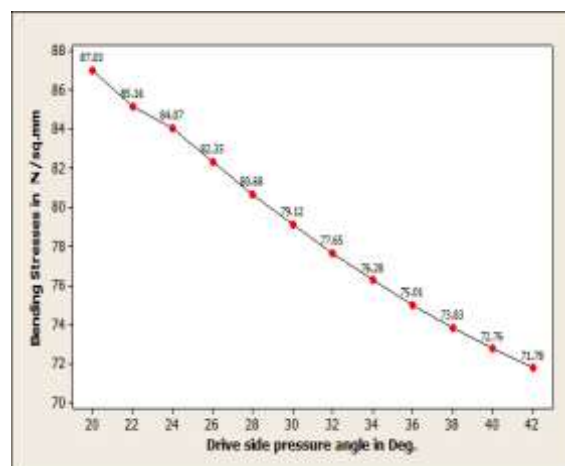


Fig. 7 Variation of Bending Stresses with Pressure angle on Drive side

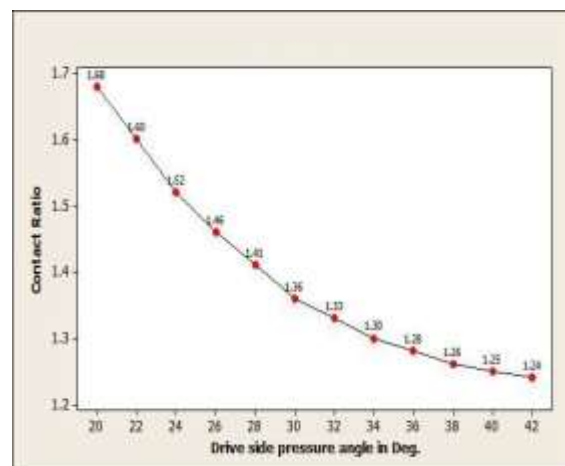
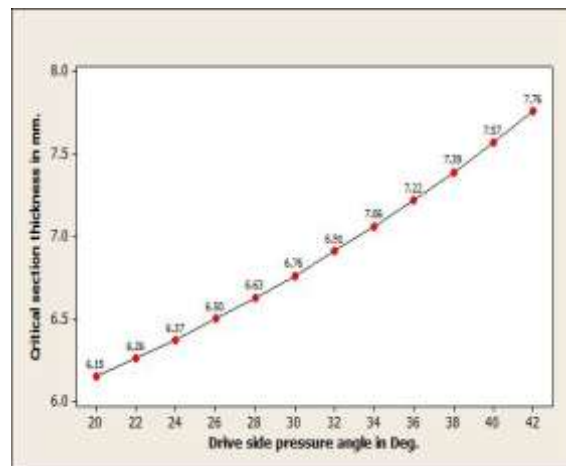
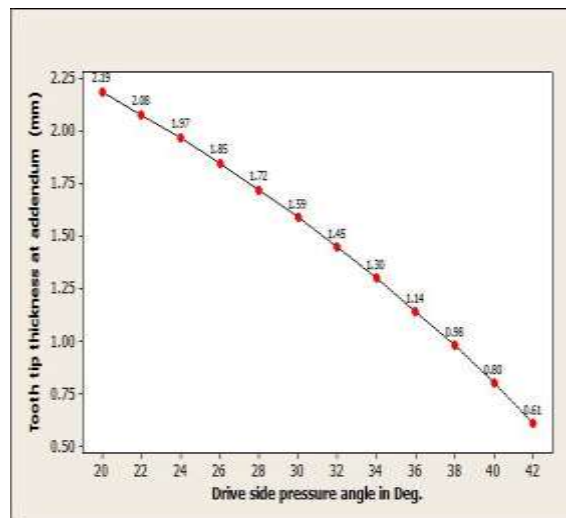


Fig. 8 Variation of Contact Ratio with Pressure angle on Drive side





**Fig. 9 Variation of Critical Thickness with Pressure angle on Drive side**



**Fig. 10 Variation of Tooth tip Thickness with Pressure angle on Drive side**

## V. Bending Stress analysis of Symmetric and Asymmetric involute Spur gear by FEA Method

The method developed to find out bending stresses theoretically by using modified ISO method is effective and fairly accurate. But the state of stress in a gear tooth are of three dimensional in nature and stress conditions are not readily amenable to theoretical analysis and required technique of Finite Element Analysis and experimental investigation for reliable analysis.

Finite element method is a powerful method for determining accurate bending stresses. The tooth bending stresses in Asymmetric Involute spur gear and symmetric Involute spur gear has been estimated using ANSYS software. The gear profile has been developed in CATIA V5 R15 [14] for different gears with same parameters like module and number of teeth but different pressure angle combinations (Design-I, Design-II and Design-III). Fig. 11 shows the Loading and boundary conditions applied to a single tooth. Stress plots have been shown in the figures 12, 13 and 14.

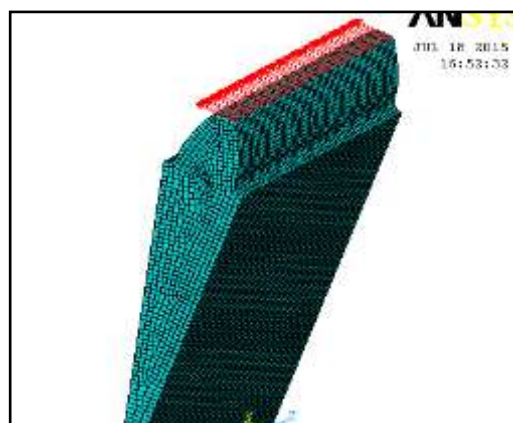


**Fig. 11 Boundary conditions and point of loading**

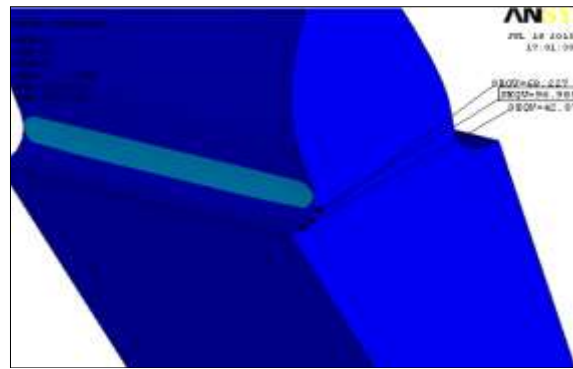


**Fig. 12 von Mises stress distribution in 3 dimensional models for Design-I**

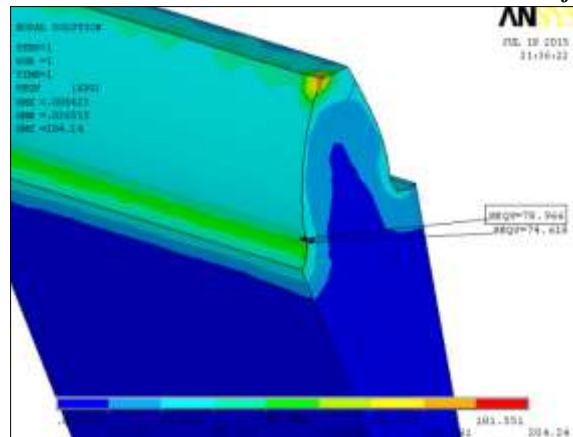


**Fig. 13 von Mises stress distribution in 3 dimensional models for Design-II**

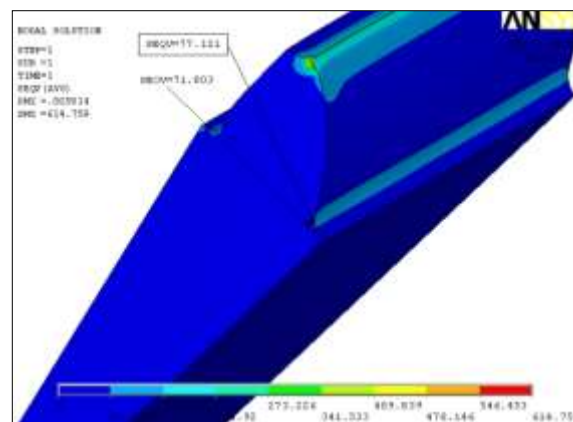


**Fig. 14 von Mises stress distribution in 3 dimensional models for Design-III**

## VI. Bending Stress analysis of Symmetric and Asymmetric involute Spur gear by Experimental Method

Photoelasticity is a non-destructive, whole-field, graphic stress-analysis technique based on mechanical property called birefringence, possessed by many transparent polymers. Combined with other optical elements and illuminated with an ordinary light source. A loaded photo elastic specimen exhibits fringe patterns that are related to the difference between the principal stresses in a plane normal to the light propagation direction. The method is used primarily for analyzing two dimensional plane problems. A method called stress freezing allows the method to be extended to three dimensional problems [15][16].

When the gear is subjected to a transmitted load, the stress condition near the area of contact and the tooth root are neither plane stress nor plane strain but are three dimensional in nature [17]. Besides it is very complex and tedious to carry out 2D photoelastic stress analysis. Therefore even though stress distribution in static condition is two dimensional, 3D photo-elastic stress analysis has been carried out to determine bending stress at the critical section. Here gear sets with Design-I, Design-II and Design-III specifications only have been considered for experimental analysis. The results of analysis are compared with those obtained by theoretical analysis and FE analysis to predict the error between these methods.



Following steps have been followed to carry out the bending stress analysis.

1. Manufacturing a pair of Asymmetric and Symmetric involute Spur Gear [18-21]  
As no standard hobs are available to manufacture asymmetric involute spur gear, a special hob has been designed and manufactured as shown in Fig. 15. Instead of traditional gear design approach, the alternative Direct Gear Design Approach has been used to manufacture asymmetric gear. Fig. 15 shows a hob with  $25^{\circ}$ - $20^{\circ}$  pressure angle. A gear with  $30^{\circ}$ - $20^{\circ}$  pressure angle has been manufactured by Wire Cutting method.
2. Preparing a photoelastic model
3. Stress Freezing
4. Slicing a model
5. Experimental Observations



**Fig. 15 Developed hob with  $25^{\circ}$ - $20^{\circ}$  pressure angle**

Fig. 16 shows the loading frame with gears, load applied and loading arm. To simulate the actual working conditions, the rotation of the prototype gear has been restricted. The stress freezing is carried out in a stress freezing oven. The slices are cut by using horizontal milling machine. At the critical section of marked tooth (critical section) on each slice, the isochromatic fringes were observed by using circular Polariscope arrangement. All the values of fringe order were noted down. The fig. 17, fig. 18 and fig. 19 show the longitudinal slices as observed under circular polariscope arrangement. The stresses developed in each slice at the critical section of marked tooth have been calculated using Tardy's compensation method [22-23]. The standard chart of Fringe color-Fringe Order has been used to find the fringe order corresponding to the color of the isochromatic fringes obtained on the slices [24]. It is observed that the color of fringe is between First and Second purple fringe (Tint of Passage) [25].



**Fig. 16 Loading Fixture**

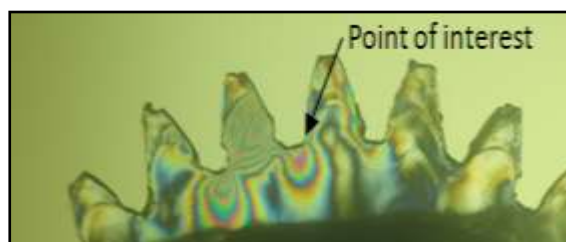


**Fig. 17 Isochromatic fringe pattern for Symmetric gear Design-I ( $20^{\circ}$ - $20^{\circ}$ ), Module 3mm,  $z_p=28$**

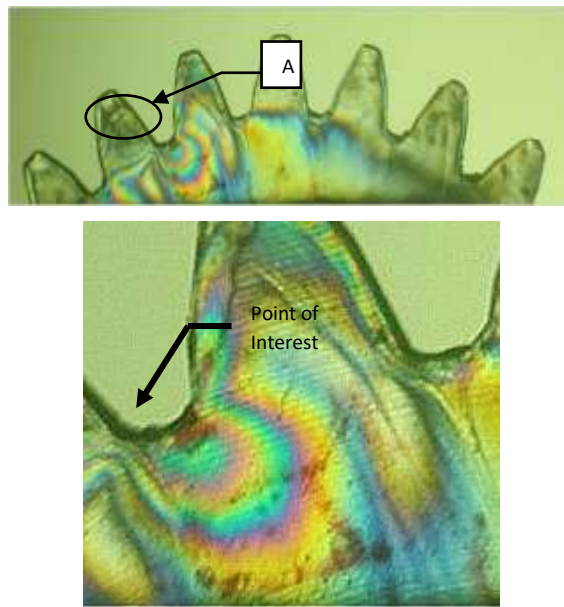


Fig. 18 Exaggerated view of A

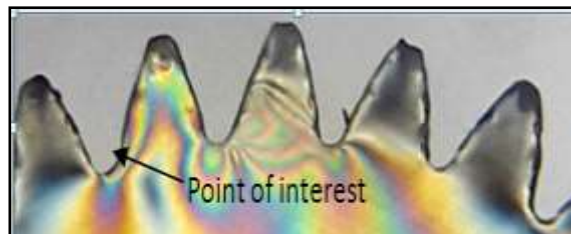


Fig. 19 Isochromatic fringe pattern for Asymmetric gear Design-III ( $30^{\circ}$ - $20^{\circ}$ ) Module 3mm,  $z_p=28$

Table 1 shows, bending stress values at Drive side for Design-I, Design-II and Design-III specifications. It also shows the error between the stresses obtained by theoretical, FEA and experimental methods.

Table 1 Error analysis between theoretical, FEA and experimental method

	Pinion Design	Stresses in pinion N/mm <sup>2</sup>			% Error	
		A Theo.	B FEA	C Exptl .	C & A	C & B
1	Design-I	87.03	96.985	94.68	8.1	2.4
2	Design-II	82.73	78.966	79.00	3.6	.04
3	Design-III	79.12	77.121	70.41	11	8

## VII. Parametric analysis of Asymmetric and Symmetric involute spur gear

Since the bending stresses in asymmetric and symmetric involute spur gear are influenced by parameters such as module, number of teeth, width of a gear and pressure angle, a parametric analysis is carried out to predict it. To carry out this analysis a Computer program in C++ has been developed and used for the purpose. Sample results are shown in Table No. 2

**Table 2 Parametric analysis of symmetric and asymmetric spur gear by varying face width**

	Drive side Pressure angle, $\alpha_d$	Coast side pressure angle, $\alpha_c$	Pinion Width, mm	Bending stress, N/mm <sup>2</sup>	% Reduction in Bending Stress.
1	20	20	36	60.43	8.32 %
	38	20	28	65.92	
2	20	20	32	67.99	8.00 %
	38	20	25	73.83	
3	20	20	32	67.99	2.00 %
	30	20	28	69.64	
4	20	20	28	77.70	06 %
	38	20	25	73.00	

### VIII. Weight Analysis of Asymmetric and Symmetric Involute Spur Gear

Almost all automobiles have a gearbox. The weight and size reduction of the gear box is significant in the general weight reduction of the vehicle and is highly desired. It is achievable with optimum cost without affecting the quality and reliability. It is possible to build up gear boxes by the design of asymmetric gears with low weight to torque ratio. This will also help to reduce the cost of gear box with asymmetric gears. As mentioned above, the asymmetric involute spur gears help to provide extremely low weight to torque ratio, weight comparison between symmetric and asymmetric involute spur gear has been carried out for different combinations of pressure angles, module and number of teeth. Referring to the results of parametric analysis, the gears with almost same bending stress values are chosen and modelled in CATIA and the weight of each gear is measured to get percentage weight reduction achieved by asymmetry. Table 3 and Table 4 shows percentage reduction in weight by varying different parameters of asymmetric involute spur gears and symmetric involute spur gears.

**Table 3 Weight Analyses of Symmetric and Asymmetric Spur gear**

P kW	$\alpha_d$	b mm	m mm	$Z_p$	$\sigma_b$ N/mm <sup>2</sup>	Wt in Kg.	% reduc <sup>n</sup> in wt.
10	20°	30	3.5	12	150	.227	34 %
	25°		3.0	12	193	.150	
2	20°	18	2.0	12	158	.035	31%
	38°		1.75	12	173	.024	
10	20°	30	4	32	35	2.77	44%
	38°		3	32	52	1.51	

### 9. Conclusions

Based on the work carried out, following conclusions have been made:

There is a fairly good agreement between theoretical, experimental and FE results (Table 1)

As pressure angle increases, the bending stresses reduce. (Figure 6)

While maintaining maximum bending stress, a substantial weight reduction can be achieved using asymmetric gear instead of symmetric one. (Table 3)

Experimental verification of bending stresses for three different designs using 3D photoelasticity is satisfactory.

### Nomenclatures

1.  $Z_p$  Number of teeth on pinion
2.  $Z_g$  Number of teeth on gear
3.  $\alpha_d$  Drive side pressure angle in degree
4.  $\alpha_c$  Coast side pressure angle in degree
5.  $d_1$  Pitch circle diameter of pinion
6.  $d_2$  Pitch circle diameter of gear
7.  $r_{bd}$  Base circle radius of pinion on drive side
8.  $r_{bc}$  Base circle radius of pinion on coast side
9.  $R_{bd}$  Base circle radius of gear on drive side
10.  $R_{bc}$  Base circle radius of gear on coast side
11.  $r_a$  Addendum circle radius of pinion
12.  $R_a$  Addendum circle radius of gear
13.  $\alpha_{ac}$  Central angle subtended by Coast side profile
14.  $\alpha_{ad}$  Central angle subtended by Drive side profile
15.  $h_{ao}$  Tool addendum factor
16.  $P$  Power transmitted
17.  $n_p$  Pinion RPM
18.  $F_t$  Tangential force
19.  $p$  Circular pitch
20.  $\alpha_p$  Load angle.
21.  $S_f$  Critical section thickness mm
22.  $CD$  Center Distance in mm
23.  $b$  Face width of gear in mm
24.  $\sigma_b$  Bending stress

### References

- [1] M. R. Ayatollahi, M. Dehghany, M. M. Mirsayar, (2013) "A Comprehensive photoelastic study for Mode-I sharp V-notches", *European Journal of Mechanics A/Solids*, pp. 216-230
- [2] M. R. Ayatollahi, M. Dehghany, M. M. Mirsayar, (2011) "Experimental determination of stress field parameters in bi-material notches using Photoelasticity", *Materials and Design*, pp. 4901-4908
- [3] M. M. Mirsayar, A. T. Samaei (2013) "Photoelastic study of bi-material notches: Effect of mismatch parameters", *Engineering Solid Mechanics*, pp. 21-26.
- [4] J.I. Pedrero and A. Reuda ,(1997) "Determination of ISO tooth form factor for involute and spur gear," *Mechanism and Machine Theory*, 34, pp. 89-103,.
- [5] A. L. Kapelewich, (2007)"Direct Design for High Performance Gear transmissions", *Gear Solutions*, pp. 22-31.
- [6] V. Spitas, Th. Costopoulos,(2009) "Reduction of gear fillet stresses by using one-sided involute asymmetric teeth, 44, pp. 1524-1534.
- [7] A. L. Kapelewich,(2007) "Applications of gears with asymmetric teeth in turbo prop engine gear box", *"International Design Engineering Technical Conferences"*, pp. 1-8.
- [8] Adrian GHIONE, "Utilization Of Some Computer Assisted Techniques In Generating And Study Of Hypocycloidal Flanks Of The Spur Gear Teeth Stress", pp. 119-126.
- [9] S. Barone, (2001)"Gear Geometric Design by B-Spline Curve Fitting and Sweep Surface Modelling", *Engineering with Computers*, Volume 17, Issue 1, pp 66-74,.
- [10] Faydor L. Litvin,(1999) "Asymmetric Modified Spur Gear Drives: Reduction of noise, Localization of Contact Simulation of Meshing and Stress Analysis", *Computer Methods in Applied Mechanics and Engineering*, 188, pp.363-390.
- [11] Gang Deng, (2003) "Bending Load Capacity Enhancement Using An Asymmetric Tooth Profile", *JSME International Journal*, pp. 1171-1177.
- [12] Kadir Cavdar, Fatih Karpat, Fatih C. Babalik, (2005)",Computer Aided Analysis of Bending Strength of Involute Spur Gear with Asymmetric Profile", *ASME Journal*, 127, pp.477-484.
- [13] J. L. Moya, A.S. Machado,(2010) "A Study in Asymmetric Plastic Spur Gears", *Gear Technology*, pp 34- 39.

- [14] Flavia Chira, (2007) "Modeling of the Asymmetric gears using applications in MATLAB & Auto LISP", *Annals of Oradea University*, FMTE, Vol.VI.
- [15] K. M. Hung, C. C. Ma, (2003) "Theoretical analysis and digital Photoelastic measurement of circular disks subjected to partially distributed compressions", *Technical Note on Experimental Mechanics*, Volume 43, Issue 2, pp 216-224.
- [16] R. L. Burguete, E. A. Patterson,(1997) "A photoelastic study of contact between a cylinder and a half-space", *Experimental Mechanics*, Volume 37, Issue 3, pp 314-323.
- [17] Jian D. Wang, Ian M.Howard, (2006)"Error analysis on finite element modeling of involute spur gears". *Journal of mechanical design*, 128, pp.90-95.
- [18] R. E. Kleiss, A. L. Kapelevich, N. J. Kleiss Jr., (2001)"New Opportunities with Molded gears", *AGMA Fall Technical Meeting*, Detroit, , (01FTM9) pp.1-9.
- [19] Alex Kapelevich, Thomas McNamara, (2003)"Direct Gear Design– for Optimal Gear Performance", *SME*.
- [20] A. L. Kapelevich, (2010) "Measurement of directly designed gears with symmetric and asymmetric teeth", *International Conference on Gears, Garching near Munich, Germany*, pp. 60-65.
- [21] A.L. Kapelevich, Y.V. Shekhman, (2010) "Fabrication of Directly Designed Gears with Symmetric And Asymmetric Teeth", presented at the *International Conference on Gears, Garching near Munich, Germany*, pp. 86-91.
- [22] J. W. Dalley and W. F. Riley, '(1978) *Experimental Stress Analysis*' Tata-McGraw Hill.
- [23] L. S. Srinath and M. R. Raghava, (1984) '*Experimental stress analysis*, Tata-McGraw Hill.
- [24] M. Allison, E. J. Hearn, (1980) "A new look at the bending strength of gear teeth, *Experimental Mechanics*", Volume 20, Issue 7, pp 217-225.
- [25] N.S.Dharashivkar,Dr.V.B.Sondur,Mr. K.D.Joshi ,(2016) „3D photoelastic and finite element analysis of Asymmetric Involute spur gear , IEEE-ICEEOT.